

# Rho mediates calcium-dependent activation of p38 $\alpha$ and subsequent excitotoxic cell death

Maria M Semenova<sup>1,4</sup>, Anu M J Mäki-Hokkonen<sup>1,4</sup>, Jiong Cao<sup>1,4</sup>, Vladislav Komarovski<sup>1</sup>, K Marjut Forsberg<sup>1</sup>, Milla Koistinaho<sup>1,2</sup>, Eleanor T Coffey<sup>3</sup> & Michael J Courtney<sup>1,3</sup>

Excitotoxic neuronal death contributes to many neurological disorders, and involves calcium influx and stress-activated protein kinases (SAPKs) such as p38 $\alpha$ . There is indirect evidence that the small Rho-family GTPases Rac and cdc42 are involved in neuronal death subsequent to the withdrawal of nerve growth factor (NGF), whereas Rho is involved in the inhibition of neurite regeneration and the release of the amyloidogenic A $\beta$ <sub>42</sub> peptide. Here we show that Rho is activated in rat neurons by conditions that elevate intracellular calcium and in the mouse cerebral cortex during ischemia. Rho is required for the rapid glutamate-induced activation of p38 $\alpha$  and ensuing neuronal death. The ability of RhoA to activate p38 $\alpha$  was not expected, and it was specific to primary neuronal cultures. The expression of active RhoA alone not only activated p38 $\alpha$  but also induced neuronal death that was sensitive to the anti-apoptotic protein Bcl-2, showing that RhoA was sufficient to induce the excitotoxic pathway. Therefore, Rho is an essential component of the excitotoxic cell death pathway.

Glutamate-induced excitotoxicity is a form of neuronal death that affects various brain regions following ischemia or in other neurodegenerative conditions<sup>1</sup>. Although it is clear that calcium influx is a key event, this has not been a useful basis for therapeutic intervention. The mechanisms by which calcium activates the downstream effectors, SAPKs<sup>2-4</sup>, have remained obscure. These kinases have also been implicated in physiological functions<sup>5-7</sup>, and so they might also be unsuitable as drug targets. This emphasizes the importance of identifying the pathway that mediates calcium-evoked SAPK activation, as this pathway might provide a rich source of targets for therapeutic intervention. The Rho family of GTPases includes cdc42, Rac and Rho, which are vital for the organization of the actin cytoskeleton. Cdc42 and Rac are also activators of the c-jun N-terminal kinase (JNK) and p38 SAPKs. The overexpression of dominant-negative forms of cdc42 and Rac is reported to protect neurons against the withdrawal of trophic support, indicating that Rac/cdc42-associated proteins might contribute to neuronal death resulting from such withdrawal<sup>8</sup>. By contrast, the experiments with bacterial toxin inhibitors of the Rho family show that neuronal survival requires activity of cdc42 and Rac but not Rho<sup>9</sup>. Rho is known to selectively activate p38 $\gamma$  but not p38 $\alpha$  in cell lines<sup>10</sup>. Dynamic rearrangements of actin mediate growth cone behavior and regulate dendritic spine morphology and overall process outgrowth, and disruption of Rho GTPase signaling is thought to contribute to mental disorders as a result of interrupting these processes<sup>11</sup>. Rho has been implicated in the inhibition of neurite regeneration<sup>12,13</sup> and the release of the amyloidogenic A $\beta$ <sub>42</sub> peptide<sup>14</sup>. Rho is regulated by calcium in the brain of *Xenopus*<sup>15</sup>, but the

relationship between Rho activity or function and the neuronal response to toxic levels of calcium has not previously been explored. Here, we provide evidence that Rho GTPase is an essential component that links glutamate-induced calcium elevation to p38 $\alpha$  activation and subsequent p38 $\alpha$ -dependent excitotoxic neuronal death<sup>4</sup>.

## RESULTS

Glutamate, the main excitatory neurotransmitter of the brain, is responsible for neuronal cell death in ischemia, and might also contribute to other neurodegenerative conditions. The treatment of cerebellar granule neurons with glutamate induces apoptosis, with many of the morphological and biochemical features of excitotoxic neuronal death in the brain, through a pathway that requires p38 $\alpha$  (ref. 4). Glutamate activated p38 with a characteristic rapid timecourse (Fig. 1a,b). Studies using *Xenopus* have shown that calcium regulates Rho both in oocyte wounds and in the brain<sup>15,16</sup>. As glutamate-induced activation of p38 $\alpha$  in primary cultured neurons depends on extracellular calcium and the calcium-permeable *N*-methyl-D-aspartate (NMDA) receptor channel<sup>4</sup>, we investigated whether Rho contributes to this response. Under physiological conditions, the C3 exoenzyme specifically ADP-ribosylates RhoA, B and C without affecting related G proteins, and thereby specifically prevents Rho from interacting with its effectors<sup>17,18</sup>. As the C3 exoenzyme is expressed from a plasmid and its neuronal transfection efficiency is low, we used an epitope-tagged p38 co-transfection assay, which we previously validated in this system<sup>4</sup>, to evaluate the effects of C3 on glutamate-evoked activation of p38 in the C3-transfected subpopulation of neurons. Transfection of

<sup>1</sup>Department of Neurobiology, A.I. Virtanen Institute, University of Kuopio, Kuopio FIN 70211, Finland. <sup>2</sup>Medeia Therapeutics Ltd, Mikrokatu 1, FI-70211 Kuopio, Finland. <sup>3</sup>Turku Centre for Biotechnology, Åbo Akademi University and University of Turku, Turku FIN-20521, Finland. <sup>4</sup>These authors contributed equally to this work. Correspondence should be addressed to M.J.C. (courtney@messi.uku.fi).

Received 27 December 2006; accepted 16 February 2007; published online 18 March 2007; doi:10.1038/nn1869

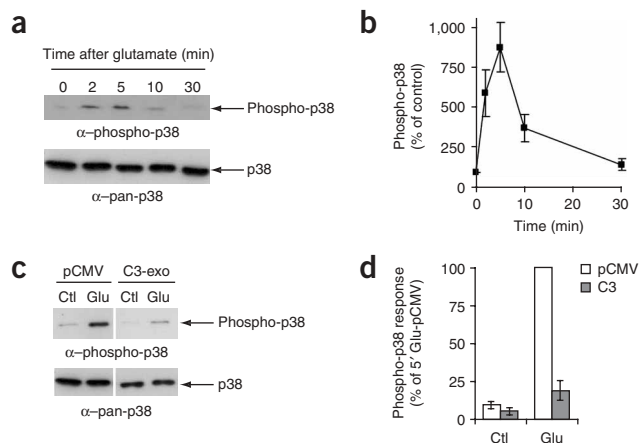


**Figure 1** Glutamate-evoked activation of p38 $\alpha$  SAPK is inhibited by the Rho inhibitor C3-exoenzyme. **(a)** Cerebellar granule neurons were stimulated with glutamate for the times indicated, and activation of p38 was assessed by immunoblotting with phospho-p38 antibody (upper panel), and equal loading checked with pan-p38 antibody (lower panel). **(b)** Mean  $\pm$  s.e.m. of replicates as in **a** ( $n = 3$ ). **(c)** Neurons were co-transfected with pEBG-p38 (encoding GST-p38) and either empty vector (pCMV) or C3 exoenzyme (C3 exo) as shown, stimulated with glutamate (Glu) or left unstimulated (Ctl) and phospho-p38 and total GST-p38 bound to glutathione beads was detected as in **a**. **(d)** Mean  $\pm$  s.e.m. ( $n = 3$ ) of replicates as in **c**. Activation of p38 by glutamate was significantly different in the presence of C3 from its absence by paired  $t$ -test ( $P < 0.005$ ).

neurons with C3 toxin prevented glutamate-evoked activation of co-transfected p38 $\alpha$  (Fig. 1c,d). One simple explanation for this could be that Rho regulates the glutamate-evoked calcium response. However, C3 had no effect on the glutamate-evoked changes in free [Ca<sup>2+</sup>] (Supplementary Fig. 1 online), indicating that it is the calcium-mediated activation of p38 $\alpha$  that requires Rho.

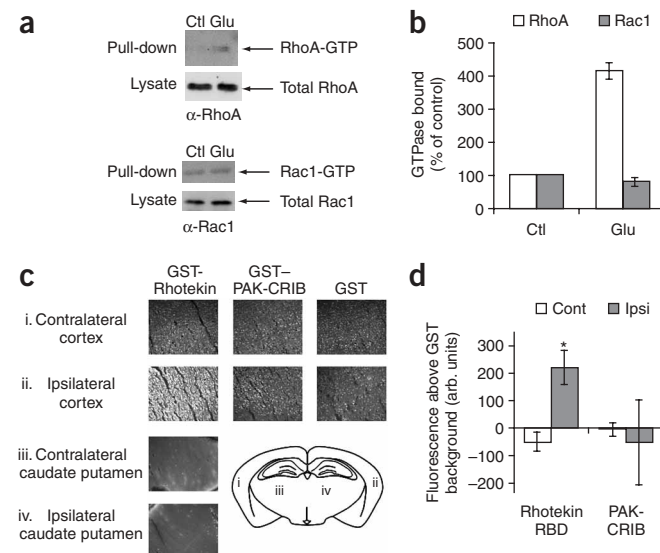
This indicates that either glutamate activates p38 $\alpha$  as a result of Rho activation, or that glutamate-induced activation of p38 $\alpha$  depends on pre-existing Rho activity. Rho activity can be measured by pull-down assay with recombinant rhotekin-RBD (Rho-binding domain of Raf) immobilized on beads. This sequence selectively sequesters activated, GTP-bound Rho in cell lysates<sup>19</sup>. Using this assay, we detected a significant increase in Rho activity after stimulation with glutamate for 3 min (Fig. 2a,b). This time point preceded the peak of glutamate-

evoked p38 activity (Fig. 1a,b). The related G-protein Rac has been implicated in some forms of neuronal apoptosis<sup>8</sup> and can regulate both SAPKs and Rho<sup>20</sup>. However, using a pull-down assay with a recombinant fusion protein containing the Cdc42/Rac interactive binding (CRIB) domain of p21-activated kinase (PAK)<sup>21</sup>, we did not detect any Rac activation at 3 min or at later times (Fig. 2a,b and Supplementary Fig. 2 online). Together with the ability of C3 to inhibit the activation of p38 $\alpha$ , these data are consistent with the idea that glutamate activates p38 $\alpha$  as a result of Rho activation.

Glutamate was used here as a model for excitotoxicity, which contributes to neurological conditions such as cerebral ischemia. We sought to address whether our findings in cell culture were relevant to excitotoxicity in brain disease. It is thought that p38 is important in cerebral ischemia, but whether Rho is involved has not been considered. We found that the standard rhotekin pull-down method, which is useful for large cell cultures (Fig. 2a), is not sufficiently sensitive to be used to analyze samples from ischemic mouse brains because the material is limited. Therefore, we applied the Rho activity staining method<sup>15</sup>. This method is based on the same principle as the pull-down method (that only active Rho binds rhotekin-RBD). Using this method, we found increased binding only in the ischemic hemisphere. As a control, binding of PAK-CRIB, which detects active Rac, was low and did not increase (Fig. 2c,d). Similarly, we found no differences between ipsilateral and contralateral rhotekin binding in mid-brain regions (Fig. 2c). This indicates that an excitotoxic stimulus leads to the activation of Rho both in purified neuronal culture and in an animal model of cerebral ischemia.

Our conclusion that Rho activates p38 $\alpha$  is surprising, as many reports have failed to detect Rho-mediated activation of p38 $\alpha$ . Although our data indicate that Rho might be necessary for glutamate-evoked p38 $\alpha$  activation, this does not mean that activation of Rho is sufficient to activate p38 $\alpha$ . Furthermore, the previously published experiments were carried out on cell lines. Therefore, we investigated whether active Rho was sufficient to activate p38 $\alpha$  and also whether Rho-mediated p38 $\alpha$  activation is a specific property of primary cultured neurons. We first transfected brain-derived neuro2A cells with p38 $\alpha$  and either empty vector or the constitutively active Rho mutant RhoA-Q63L (GTPase negative). The presence of active Rho failed to increase p38 $\alpha$  activation in these cells (Fig. 3a); rather, p38 $\alpha$  was inhibited. Subsequently, we transfected primary cultured cerebellar

**Figure 2** Excitotoxic stress activates Rho in cerebellar granule neuron cultures and in mouse brain. **(a)** Neurons were left unstimulated (Ctl) or stimulated with glutamate for 3 min (Glu). Activated GTP-bound Rho and Rac were sequestered from cell lysates with immobilized recombinant rhotekin-RBD and PAK-CRIB, respectively, and detected by immunoblotting with RhoA and Rac1 antibodies (Pull-down). Equal presence of RhoA and Rac1 in lysates was determined by immunoblotting cell lysates with the same antibodies (Lysate). **(b)** Mean  $\pm$  s.e.m. of replicates as in **a**.  $n = 3$  and 5 for Rho and Rac, respectively. The signal for RhoA but not Rac1 was significantly different between control and glutamate by paired  $t$ -test,  $P < 0.01$ . **(c)** Rho is activated in ischemic (ipsilateral) cortex of adult mouse 30 min after middle cerebral artery occlusion. Fixed brain sections from ipsilateral and contralateral cortex, and caudate putamen as control brain region, were stained with GST-rhotekinRBD, GST-CRIB or GST alone for active Rho, active Rac/cdc42 and background signal, respectively. Staining was visualized by fluorescent tyramide-based amplification. The scheme shows the locations of the brain regions from which the images were obtained. **(d)** Mean  $\pm$  s.e.m. of replicates as in **c** (contralateral, cont and ipsilateral, ipsi;  $n = 4$ ). \* denotes significant difference between ipsilateral and contralateral cortex by paired  $t$ -test ( $P < 0.01$ ).



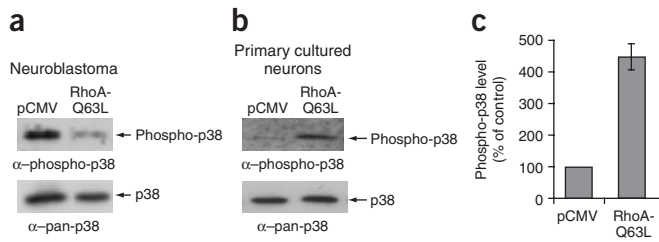


**Figure 3** Rho activates p38 $\alpha$  in cerebellar granule neurons but not Neuro2A neuroblastoma cells. **(a)** Neuro2A cells were transfected with pEBG-p38 $\alpha$  and empty vector (pCMV) or RhoA-Q63L (GTPase negative) active mutant, and p38 activity and total p38 were detected by immunoblotting. Active RhoA failed to activate p38 $\alpha$  in this cell type. **(b)** Primary cultured cerebellar granule neurons were transfected with plasmids as in **a**, and p38 activity was measured. Active RhoA could activate p38 $\alpha$  in these neurons. **(c)** Mean  $\pm$  s.e.m. of replicates as in **b** ( $n = 4$ ; significant difference from control,  $P < 0.005$ ).

granule neurons with p38 $\alpha$  and either empty vector or RhoA-Q63L. In these cells, RhoA-Q63L produced strong activation of p38 $\alpha$  (Fig. 3b,c). These results indicate that active Rho is sufficient to activate p38 $\alpha$ , but only in the primary cultured neurons. This is consistent with our previous observation that even in neuroblastoma and other neuron-like cell lines, the SAPK pathways show distinctly non-neuronal behavior<sup>5</sup>.

Activation of p38 $\alpha$  is required for glutamate-induced apoptosis of cerebellar granule neurons<sup>4</sup>. Therefore, we speculated that Rho might also be required for this excitotoxicity. To test this possibility, we transfected cells with empty vector or C3 toxin together with GFP transfection marker, and we treated the cultures with glutamate. Pyknosis is an early indicator of glutamate-induced death in cerebellar granule neurons, preceding loss of membrane integrity by several hours<sup>4</sup>. We therefore assessed apoptosis by pyknosis of GFP-positive neurons<sup>4</sup>. This showed that C3 could prevent the excitotoxic cell death (Fig. 4a,b). We found similar results using a dominant-negative form of Rho, RhoA-T19N (Fig. 4c). By contrast, the equivalent dominant-negative form of Rac, Rac1-T17N, which protects NGF-deprived rat sympathetic neurons<sup>8</sup>, had no effect on glutamate-evoked pyknosis (Fig. 4d).

Together with the lack of Rac activation (Fig. 2 and Supplementary Fig. 2), these results indicate that Rac is not involved in the glutamate-evoked response described here. Instead, they indicate that Rho is necessary for glutamate-evoked pyknosis, although they have no bearing on whether Rho activation is sufficient for pyknosis. Active Rho is sufficient to activate p38 $\alpha$  (Fig. 2) and overexpression of constitutively active MKK6, a p38-specific activator, is sufficient to induce Bcl-2-sensitive pyknosis (Supplementary Fig. 3 online). Therefore, we transfected active Rho or empty vector together with a transfection marker into

either cerebellar granule neurons or, as a negative control, neuroblastoma cells that did not exhibit Rho-induced activation of p38 (Fig. 4e). Active Rho induced pyknosis only in the primary cultured neurons, and co-expression of Bcl-2 prevented this response, as it does for glutamate-induced death in this system<sup>4</sup>.

Our evidence that Rho helps to cause excitotoxic death derives from a cerebellar granule neuron model of p38-dependent excitotoxicity. There is evidence that p38 also contributes to excitotoxicity in cerebral ischemia, and the neurons of the cerebellum are also sensitive to excitotoxicity *in vivo*. We investigated directly whether Rho also contributes to excitotoxic signaling in other neurons that are sensitive to excitotoxicity. NMDA induces excitotoxic cell death of cultured cortical and hippocampal neurons. We therefore transfected cultures of cortical and hippocampal neurons with a viability marker with or without an expression plasmid for C3-exoenzyme. NMDA treatment resulted in a substantial loss of transfected neurons, and this was partially prevented by co-expression of C3 exoenzyme (Fig. 5a,b). The possible contribution of Rho to NMDA-evoked p38 activation in cortical neurons was evaluated as in Figure 1. C3 reduced NMDA-evoked phospho-p38 responses when compared to cultures transfected with empty vector (Fig. 5c,d). C3 expression did not reduce NMDA-evoked calcium responses in either type of neuron (Supplementary Fig. 1 and data not shown), consistent with Rho being an intermediate between excitotoxic calcium elevation and p38, as in the cerebellar neurons (Fig. 1).

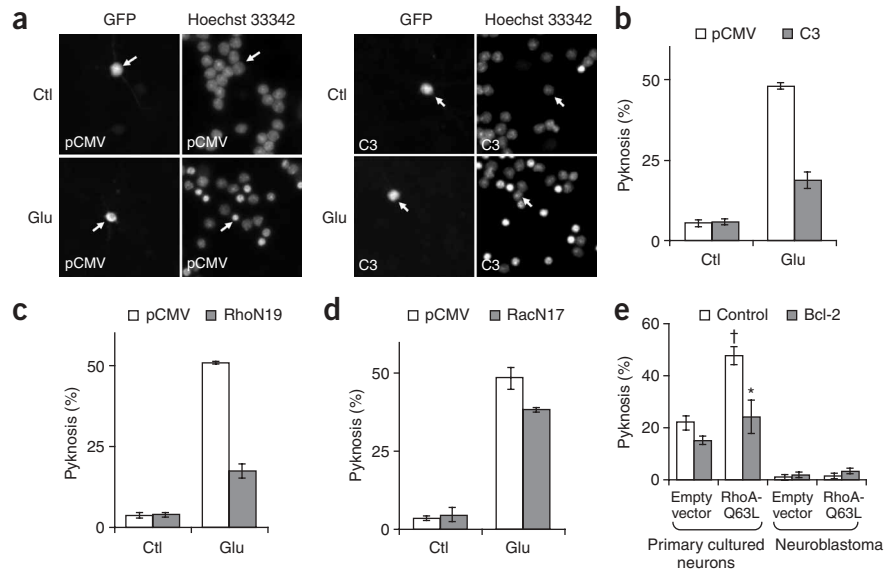


**Figure 4** The Rho inhibitor C3-exoenzyme inhibits glutamate-evoked neuronal cell death. **(a)** Neurons were transfected with pEBG-C3-exoenzyme (C3) or empty vector (pCMV) together with GFP as a transfection marker and treated with glutamate (30 min, 50  $\mu$ M). After 3 h, cells were fixed and DNA stained with Hoechst 33342, to allow assessment of pyknosis. GFP and Hoechst images are shown. C3 inhibited glutamate-induced pyknosis. **(b)** Replicates of data as in **a** (mean  $\pm$  s.e.m.;  $n = 3$ ). Paired *t*-test showed a significant difference between C3- and pCMV-transfected glutamate-treated samples ( $P < 0.001$ ). **(c)** The experiments in **a** and **b** were repeated with a dominant-negative Rho mutant, RhoA-T19N. Results are shown as mean  $\pm$  s.e.m. ( $n = 3$ ). Paired *t*-test showed a significant difference between C3- and pCMV-transfected glutamate-treated samples ( $P < 0.0005$ ). **(d)** We repeated the experiment with a dominant-negative Rac mutant, Rac1-T17N. Paired *t*-test showed no significant protection. Results are shown as mean  $\pm$  s.e.m. ( $n = 3$ ). **(e)** Neurons and Neuro2A cells (Neuroblastoma) were transfected with active Rho, RhoA-Q63L, or empty vector. In transfected neurons, pyknosis was increased by expression of active Rho, and this increase was prevented by co-expression of Bcl-2. In transfected neuroblastoma cells, active Rho had no effect on pyknosis. Means  $\pm$  s.e.m. ( $n = 6$ ) are shown. † indicates a significant difference from control without RhoA Q63L and \* indicates a significant difference from corresponding sample without Bcl-2, by *t*-test ( $P < 0.05$  or better).

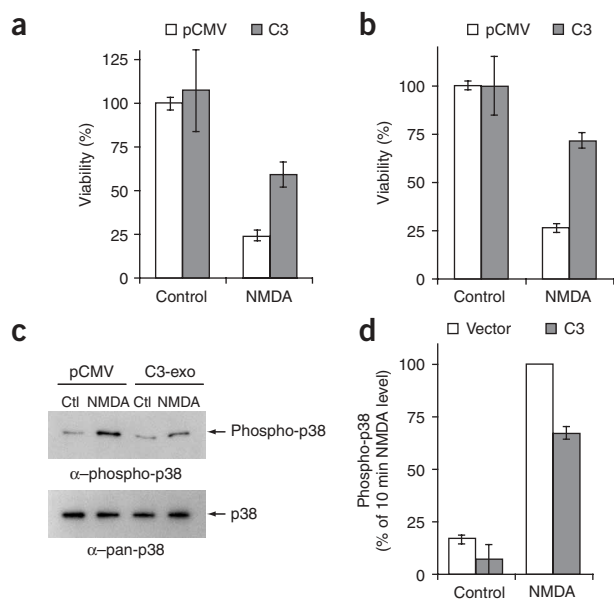


**Figure 5** Involvement of Rho in excitotoxic signaling and cell death in hippocampal and cortical neurons. **(a)** Hippocampal neurons were transfected with empty vector or C3 expression plasmid as indicated, and exposed to NMDA or left untreated. After 24 h, cell viability was assessed by the number of remaining transfected cells per microscope field normalized to the cell numbers without NMDA treatment. Means  $\pm$  s.e.m. are shown ( $n = 4$  coverslips per condition). **(b)** The experiment in **a** was repeated in cortical neuron cultures. Means  $\pm$  s.e.m. are shown ( $n = 4$ ). **(c)** Cortical neuron cultures were transfected with p38 expression plasmid and stimulated with NMDA for 10 min as indicated. p38 was purified from cell lysates and p38 activation measured as in **Figure 1c,d**. **(d)** Replicates of experiments as in **c** carried out in cortical cultures. Means  $\pm$  s.e.m. are shown ( $n = 3$ ).

Although we used a pull-down assay to show that neuronal Rho was rapidly activated by glutamate, this is a very insensitive assay and is not suitable for mechanistic investigation of the requirements of the Rho activation in primary cultures, where the material is limited. Therefore we applied the fluorescence-resonance energy transfer (FRET) probe of Rho activation, Raichu-RBD<sup>22</sup>, to the primary neuronal cultures. This probe consists of Venus (a brighter version of yellow fluorescent protein (YFP)) and cyan fluorescent protein (CFP) moieties separated by rhotekin-RBD (**Fig. 6a**). Rhotekin-RBD specifically interacts with activated forms of RhoA, RhoC and to a lesser extent RhoB<sup>23</sup> but not with related proteins<sup>24</sup>. Activation of Rho therefore leads to binding to rhotekin-RBD, increased separation of the fluorophores and consequent loss of FRET (**Fig. 6a**). We transfected cells with this probe and monitored the emission of CFP and Venus fluorescence. Activation of Rho led to a loss in FRET, seen as an increase in the CFP/YFP emission ratio (FRET ratio). Before glutamate was added, thresholded and

background-corrected ratiometric images showed that the neurons tend to exhibit higher FRET ratios at the periphery of the cell and in some but not all processes. Addition of glutamate induced a rapid rise in the FRET ratio in more central regions of the cell body (**Fig. 6b**).

The presence of the NMDA channel blocker MK-801 substantially reduced the glutamate-evoked FRET response (**Fig. 6c**). Co-transfection of C3, which ADP-ribosylates Rho and prevents it from interacting with effectors<sup>25</sup>, also substantially reduced the glutamate-evoked signal (**Fig. 6c**). These data indicated that the glutamate-evoked FRET response was dependent on NMDA receptor activity, and also on Rho activity (that is, the response represented genuine Rho activation and, like the glutamate-evoked activation of p38 $\alpha$  and subsequent cell death<sup>4</sup>, required NMDA receptors). The time-course of Rho activation was rapid and consistent with Rho being upstream of the p38 response (**Fig. 1b**).

To investigate the relationship between activation of Rho and pyknosis, we evaluated the concentration dependence of glutamate-evoked  $[Ca^{2+}]$  elevation, Rho activation, p38 activation and pyknosis. We detected  $[Ca^{2+}]$  elevation at 5  $\mu$ M glutamate, reaching a maximum at 15–50  $\mu$ M (**Fig. 7a,b**). This concentration range was sufficient to activate Rho (**Fig. 7c,d**). Activation of p38 and induction of pyknosis were detectable at 5  $\mu$ M but highest at 50  $\mu$ M (**Fig. 7e,f**). We extended the pyknosis assay to higher concentrations of glutamate and found that 50  $\mu$ M evoked the maximal response. Together, these results indicate that activation of Rho contributed to pyknosis evoked by higher concentrations of glutamate, and are consistent with inhibition

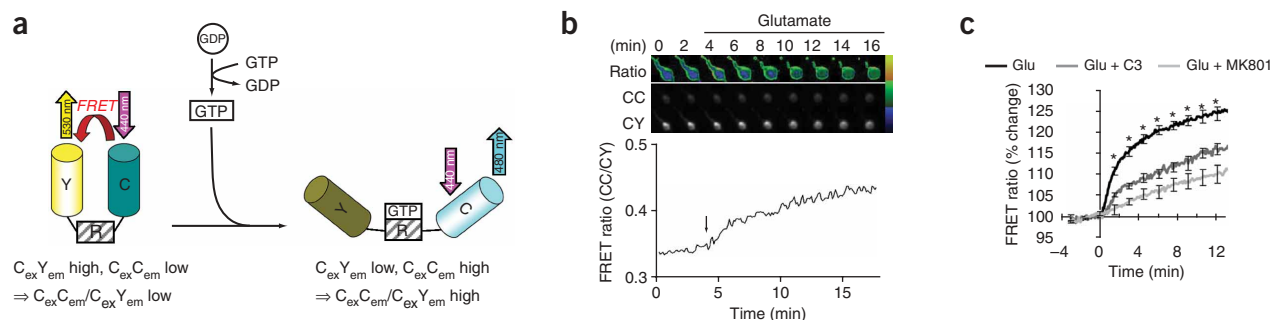


**Figure 6** FRET-based reporter of Rho activity reveals rapid glutamate-evoked activation of Rho that depends on NMDA receptors. **(a)** Raichu-RBD contains VenusYFP (Y) and CFP (C) separated by rhotekin-RBD (R). Its basal 'closed' conformation exhibits FRET. Active RhoGTP binds RBD, separating the fluorophores and reducing FRET. CC ( $C_{ex}C_{em}$ ) and CY ( $C_{ex}Y_{em}$ ) represent signals measured at emission wavelengths for CFP and YFP, respectively, when the probe is excited with light optimal for excitation of CFP. **(b)** A neuron expressing Raichu-RBD was imaged and stimulated with glutamate at 4 min. Pseudocolor CC/CY ratio images are shown in the top panel and raw CC and CY grayscale image pairs of the cell are shown in the middle panel. The bottom panel indicates the ratio of background-corrected CC and CY fluorescence signals from the region containing the neuron. Glutamate addition is indicated by the arrow. The pseudocolor bar to the right of the images indicates the change in color with increasing ratio. **(c)** Cerebellar granule neurons transfected with Raichu-RBD were stimulated with glutamate at 0 min. FRET ratio (CC/CY, as defined above) timecourses were calculated from individual cell soma, and average responses were calculated from all cells in a field. The response is substantially reduced by either co-transfection with C3 or treatment with MK-801. Means of average timecourses from four (Glu, Glu + C3) or two coverslips (Glu + MK801)  $\pm$  s.e.m. (where  $n = 4$ ) or range (where  $n = 2$ ) are shown. \* denotes significant difference between 'Glu' and 'Glu + C3' traces by *t*-test ( $P < 0.05$  or better).



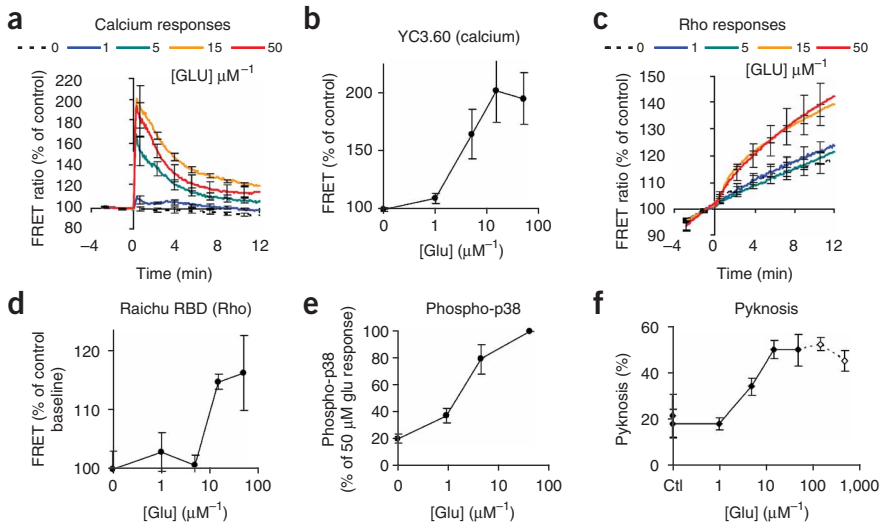


**Figure 7** Concentration dependence of glutamate-evoked changes in cytoplasmic free calcium, Rho response, p38 activation and pyknosis. **(a,b)** Glutamate increases  $[Ca^{2+}]_i$  and **(c,d)** Rho activity in neurons in a concentration-dependent manner, as measured with FRET probes YC3.60 and Raichu-RBD, respectively. Average timecourses are shown ( $n = 4-7$  coverslips). **(b,d)** The peak calcium response and Rho response above baseline 9 min after glutamate addition are shown as mean  $\pm$  s.e.m. ( $n = 4-7$  coverslips). **(e)** Concentration-dependent increase in phospho-p38 5 min after glutamate addition. Means  $\pm$  s.e.m. are shown ( $n = 3$ ). **(f)** Concentration-dependent induction of pyknosis 3 h after removal of glutamate. Concentrations above 50  $\mu M$  were tested in this experiment (open symbols and dotted lines). Ctl indicates two controls, one in which cells were incubated with MK801 in place of glutamate (lower value) and the other in which cells were left in culture medium instead of being exposed to glutamate (upper value). Means  $\pm$  s.e.m. are shown ( $n = 6$ ).

of Rho by C3 conferring only partial protection against glutamate-evoked pyknosis (**Fig. 4**).

The neurotoxicity of NMDA receptor activity is believed to result mainly from the calcium permeability of the channel. Furthermore, glutamate-evoked activation of p38 depends on extracellular calcium<sup>4</sup>. Therefore, we used Raichu-RBD to investigate whether elevation of free intracellular calcium is sufficient to activate Rho. Depolarization of the plasma membrane of cerebellar granule neurons by addition of 30 mM KCl to the extracellular medium induced a characteristic calcium response<sup>26</sup> and an increase in the FRET ratio (**Fig. 8a**, +KCl +Ca trace). Addition of KCl in the absence of extracellular calcium also

induced a small increase in the FRET ratio, possibly due to the minor osmotic stress (**Fig. 8a**, KCl -Ca). However, most of the KCl response depended on the presence of calcium. As with glutamate, if Rho activated neuronal p38 then other treatments that activate Rho would also be expected to activate p38. Exposure of neurons to 30 mM KCl also activated p38 with a timecourse similar to activation by glutamate (**Fig. 8b,c**), and KCl-evoked activation of the p38 reporter was blocked by co-transfection of C3 toxin (**Fig. 8d,e**). We also tested the effect of KCl on pyknosis. There was no significant increase in pyknosis after treatment with KCl ( $1.7\% \pm 0.3\%$  in control,  $2.5\% \pm 0.5\%$  after 30 mM KCl;  $n = 3$ ), consistent with the ability of KCl to activate trophic pathways in neurons.

To investigate how elevated calcium activates Rho, we considered Rho guanine nucleotide exchange factor (RhoGEF) and Rho GTPase-activating protein (RhoGAP) activities. Recombinant Rho was loaded with isotopically labeled  $[^3H]$ -GDP or  $[\gamma\text{-}^{32}P]$ -GTP, and incubated with control or glutamate-treated lysates in a crude lysates assay<sup>27</sup>. However, we found no glutamate-evoked change in total RhoGEF or RhoGAP activities (data not shown). Although many RhoGEFs exist, p115RhoGEF is particularly important for the regulation of Rho.  $G\alpha_{13}$  activates Rho through p115RhoGEF<sup>28</sup>, so we validated the inhibitory effect of the regulator of G-protein signaling (RGS) domain of p115RhoGEF by showing that it strongly inhibited the constitutively active  $G\alpha_{13}$ -evoked C3-sensitive SRE-reporter response (**Supplementary Fig. 4** online). The same p115RGS construct had no effect on glutamate-evoked pyknosis or glutamate-induced Rho activity, as measured by the FRET assay (**Supplementary Fig. 4**). There are also many RhoGAPs. One of them, p250RhoGAP, dissociates from NMDA receptors upon calcium-dependent activation of calcium/calmodulin-dependent kinase type 2 (CaMKII)<sup>29</sup> and is therefore also a prominent candidate

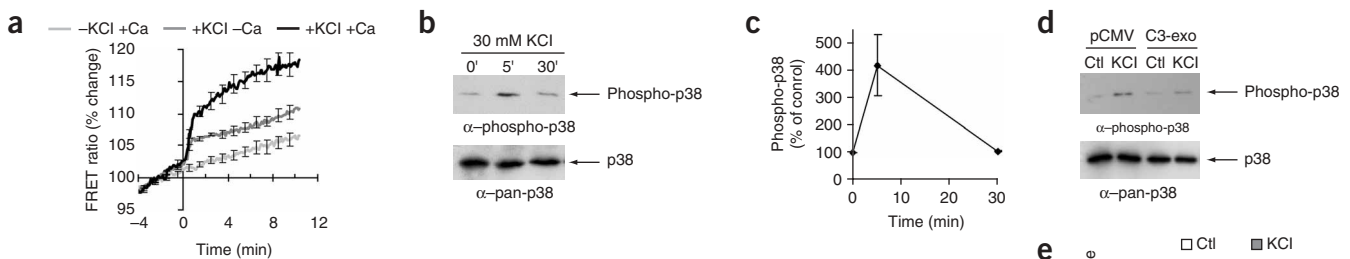


**Figure 8** Depolarization activates Rho in a manner that depends on extracellular calcium. p38 is also activated.

**(a)** Raichu-RBD-transfected neurons were exposed to 30 mM KCl in the presence (+KCl +Ca) or absence (+KCl -Ca) of 1.3 mM extracellular  $CaCl_2$ , or left untreated (-KCl +Ca). FRET ratio was monitored as in **Figure 6**, showing that KCl evokes a response that largely depends on extracellular calcium. Means  $\pm$  s.e.m. ( $n = 3-5$ ) are shown. **(b)** Neurons were treated with 30 mM KCl for times shown, in the presence of 1.3 mM  $CaCl_2$ . Activation of p38 was detected as in **Figure 1**, and pan-p38 immunoblotting revealed equal loading in all lanes. **(c)** Replicates of data in **b** are shown as mean  $\pm$  s.e.m. ( $n = 3$ ). **(d)** Neurons were co-transfected with pEBG-p38 $\alpha$  and either empty vector (pCMV) or C3 exoenzyme (C3) and depolarized (KCl) or left unstimulated (Ctl). Phospho-p38 and total GST-p38 bound to glutathione beads were detected as in **Figure 1**. **(e)** Mean phospho-p38 signals from replicates of **d** are shown  $\pm$  s.e.m. ( $n = 3$ ). Data were normalized to respective controls to highlight the impact of C3 on the KCl response, as C3 alone increased basal phospho-p38 to  $158 \pm 10\%$ .

for glutamate-evoked activation of Rho. However, a dominant negative CaMKII $\delta$  mutant had no effect on the Rho FRET response (**Supplementary Fig. 4**), and pharmacological inhibition of CaMKII did not reduce glutamate-evoked pyknosis (data not shown). Thus we can exclude p115RhoGEF and CaMKII-dependent events such as the calcium-evoked translocation of p250RhoGAP as candidate mediators of the glutamate-evoked Rho pathway.

Rho acts through downstream effectors, around 20 of which have been described<sup>18</sup>; additional effectors are still being uncovered<sup>30</sup>. Loop 6 of RhoA confers specificity for some Rho effectors<sup>31</sup>. As a result, Rho-to-Rac point mutations (D87V/D90A) in active RhoA Q63L lead to the loss of the ability of Rho to bind to the effectors Rho-kinase (Rock) and protein kinase N (PKN)<sup>31</sup>. Using the assay from **Fig. 4e**, we found that neuronal pyknosis induced by Q63L-activated RhoA was brought down to control levels when we included the Rho-to-Rac mutations (**Supplementary Fig. 5** online). This indicates that RhoA-induced pyknosis involves effectors for which loop 6 determines binding. The synthetic compound Y-27632 inhibits the kinase activity of several Rho effectors, in particular the loop 6-dependent effectors RockI and RockII<sup>32</sup>. Although Y-27632 is taken up by cerebellar granule neurons<sup>33</sup>, it had no effect on glutamate-induced pyknosis even at a concentration of 100  $\mu$ M (**Supplementary Fig. 5**). The kinase activities of RockI and II are therefore dispensable for glutamate-induced neuronal death.

## DISCUSSION

Excitotoxicity—the death of neurons induced by over-stimulation of glutamate receptors—contributes to neurological deficits in many brain regions after ischemia, traumatic brain injury and in other neurodegenerative conditions<sup>1</sup>. Most forms of excitotoxic cell death require NMDA receptors and calcium influx, but these features have not proven to be suitable drug targets. More recent evidence indicates that stress-activated protein kinases (SAPKs) are also involved<sup>2–4</sup>. In spite of their potential as novel drug targets for diseases that involve excitotoxicity, the mechanisms by which calcium overload activates these kinases remain obscure. Furthermore, these kinases have also been implicated in physiological functions<sup>5–7</sup>. SAPKs might therefore also be unsuitable drug targets, emphasizing the importance of identifying intermediates between calcium overload and SAPK activation. We have shown that Rho GTPase is required in the pathway that links calcium influx with the stimulation of the neuronal SAPK p38 $\alpha$ , and for subsequent cell death.

Rho-family GTPases are best known as regulators of the actin cytoskeleton, but two members, cdc42 and Rac, are also potent activators of SAPKs. There is indirect evidence that these proteins are involved in cell death induced by withdrawal of NGF<sup>8</sup>. The role of Rho in the regulation of SAPKs is more complex. Rho can regulate JNK in a cell-type dependent manner<sup>34</sup>. It also appears that Rho can activate the  $\gamma$ -isoform of p38, but investigations of p38 $\alpha$  indicate that this isoform is not regulated by Rho. However, our data support our proposal that Rho mediates glutamate-induced p38 $\alpha$  activation; glutamate activates p38 $\alpha$  (**Fig. 1c,d**) and no activated p38 species with a molecular weight consistent with the  $\gamma$ -isoform<sup>35</sup> was detected (**Fig. 1a**).

Most studies in neurons have focused on the potential roles of Rho proteins in growth cone and dendritic morphology and dynamics. There is considerable evidence that Rho, Rac and cdc42 have roles in these events, and disruption of Rho GTPase signaling is thought to contribute to mental disorders as a result of this function being disrupted<sup>11</sup>. It has been proposed that Rho mediates the remodeling of dendrites by glutamate. However, activation of Rho by glutamate in mammalian systems has been inferred from downstream responses

rather than measured directly<sup>36</sup>. In this study, recently developed FRET reporters permitted us to show that glutamate activates Rho in mammalian neurons with a rapid timecourse, consistent with our proposal that it mediates the rapid activation of p38 $\alpha$  by glutamate.

Few studies have addressed the potential contributions of the Rho family to neurodegeneration. Toxin-based inhibition of Rac in unchallenged neurons leads to apoptosis, whereas inhibition of Rho with C3 toxin does not reduce viability<sup>9</sup>. This is consistent with our finding that neurons had basal Rac activity and C3 toxin did not reduce viability (in fact we could not detect basal Rho activity). But the earlier report did not exclude a pro-death role for Rho, which we have revealed in this study. Furthermore, we found that glutamate selectively activated Rho but not Rac, and that mutation of Rho-specific amino acids in loop 6 of Rho to the corresponding amino acids from Rac prevented Rho-evoked pyknosis, consistent with the consequential loss of binding to Rho effectors<sup>31</sup>. Thus, Rho and Rac are clearly distinct in their regulation and contributions to cell death. It is likely that inhibition of Rho will effect the actin cytoskeleton, in turn indirectly and gradually affecting NMDA receptor localization. This might influence neuronal responses to glutamate. However, we found no inhibition of the overall NMDA receptor-evoked [Ca<sup>2+</sup>] response in neurons in which Rho was inhibited. Besides, regulation of the actin cytoskeleton has been reported to selectively affect synaptic glutamate receptor function without influencing responses to bath application of glutamate<sup>37</sup> as used here. Therefore, the neuroprotection conferred by C3 is probably not secondary to general structural rearrangements. Furthermore, the Rho activators glutamate and KCl both activated Rho and led to activation of p38 within minutes, and it is this rapid activation that was inhibited by C3 toxin. This indicates that the contribution of Rho activation to glutamate-evoked activation of p38 is rapid, rather than being a gradual response that could be expected from receptor relocalization driven by cytoskeletal rearrangements.

As depolarization with KCl also activated Rho, and Rho could induce pyknosis, it might appear surprising that KCl did not induce pyknosis. Similarly, KCl and glutamate both increased calcium influx, but only glutamate was neurotoxic. It is well known that increases in calcium evoked by NMDA receptors are more toxic than those evoked by KCl, although the explanation for this has remained elusive for decades. Our data show that the two stimuli can activate Rho similarly, but KCl produces substantially lower activation of p38 and does not evoke apoptosis. In the latter respect, the KCl response is similar to the response to 1  $\mu$ M glutamate (**Fig. 7**). KCl provides trophic support to cerebellar granule neurons, which involves activation of Akt. By contrast, glutamate treatment leads to inhibition of Akt in these neurons<sup>38</sup>. Akt can antagonize SAPK (JNK/p38) pathways through inhibitory phosphorylation of both mitogen-activated protein kinase kinases (MAP3Ks) and MAP2Ks, and can also inhibit Bcl-2-sensitive death pathways. As we are considering a p38-dependent, Bcl-2 sensitive cell death mechanism, it seems likely that the differential actions of KCl and NMDA on Akt activity could explain the survival-promoting effect of KCl, as has been previously proposed<sup>38</sup>.

We investigated the contribution of Rho to a model of glutamate-induced neuronal death that we have characterized in detail<sup>4</sup>. Excitotoxicity can affect various brain regions and contribute to different neurodegenerative conditions. The morphological and biochemical features of degenerating neurons indicate that multiple mechanisms might underlie this form of cell death even within a single brain region under a single stress, such as in ischemic cerebral cortex<sup>39,40</sup>. More effective neuroprotection will result from an understanding of different forms of neuronal cell death, which requires the use of multiple model systems. Glutamate-induced death in the cerebellar granule neuron

model depends on NMDA receptors and shares properties<sup>4,41</sup> with other examples of excitotoxic death, such as in cultured cortical neurons and in ischemic brain. These properties include lumpy chromatin condensation<sup>39,40,42</sup>, caspase independence<sup>39,41</sup>, insensitivity to inhibitors of transcription and translation<sup>43–45</sup>, sensitivity to inhibition of p38 (ref. 46), involvement of NO or neuronal nitric oxide synthase (nNOS)<sup>47,48</sup>, and sensitivity to inhibition of poly(ADP-ribose) polymerase (PARP)<sup>41</sup>. This system might therefore be useful for modeling forms of excitotoxic cell death that share these properties. In addition, we have shown that Rho is activated in the cortex after cerebral ischemia, and that inhibition of Rho reduces NMDA-evoked activation of p38 $\alpha$  and loss of viability in cultures of cortical and hippocampal neurons. Our results therefore showed an unexpected requirement for Rho GTPase in the pathway that links calcium influx with stimulation of the neuronal SAPK p38 $\alpha$  and apoptosis (**Supplementary Fig. 6** online). Rho might therefore contribute to some forms of excitotoxic cell death. Inhibition of Rho inhibition has proven to be beneficial in models of axonal regeneration<sup>12</sup> and regulation of the release of the amyloidogenic A $\beta$ <sub>42</sub> peptide from neuroblastoma cells<sup>14</sup>. In the light of the present data, Rho inhibition might also help to increase survival subsequent to excitotoxic challenge.

## METHODS

**Cell culture and cell stimulation.** We prepared and maintained primary cultures of cerebellar granule neurons as described<sup>5</sup>. We prepared cortical neurons as described<sup>7</sup> and we cultured hippocampal neurons similarly. We used neurons after 7–9 days *in vitro*. For glutamate treatment, we rinsed cultures twice in Mg-free Locke's buffer (154 mM NaCl, 5.6 mM KCl, 3.6 mM NaHCO<sub>3</sub>, 1.3 mM CaCl<sub>2</sub>, 5.6 mM D-glucose, 5 mM HEPES buffer, pH 7.4) and placed them in Locke's buffer with glutamate (50  $\mu$ M or as shown) for 30 min, or as shown. We routinely included 10  $\mu$ M glycine with glutamate as it is an essential co-agonist for the NMDA receptor. Subsequently we rinsed cells once in Locke's buffer with 1 mM MgCl<sub>2</sub> and replaced the conditioned medium for the time indicated. For NMDA treatment, we removed a portion of growth medium from cortical and hippocampal neuron cultures. We added NMDA to this medium and replaced it onto the cultures. Viability was assessed 24 h after NMDA addition. For KCl treatment, we rinsed cultures twice in Locke's buffer and placed them in the same buffer with 1 mM MgCl<sub>2</sub> and 30 mM KCl. For each stimulus, we assessed pyknosis by continuing the stimulation for 30 min, rinsing cultures once with corresponding wash buffer as above, and returning to conditioned medium for 3 h. To assess p38 activation, we stimulated cultures for 5 min or as shown in the figures, and then lysed them in laemmli sample buffer (62.5 mM Tris-HCl, pH 6.8, 1% SDS (w/v), 5% 2-mercaptoethanol, 10% glycerol (v/v) and 0.001% bromophenol blue (w/v)) for immunoblotting analysis.

**FRET-based imaging of Rho activation and [Ca<sup>2+</sup>] elevation.** We cultured neurons on 10-mm square glass coverslips and co-transfected them after 6–7 days *in vitro* with FRET reporter (Raichu-RBD<sup>22</sup>, YC2.12 or YC3.60<sup>49</sup>) and empty vector or pEF-C3 exoenzyme as indicated. The next day, we washed the coverslips once in Locke's buffer with 1 mM MgCl<sub>2</sub> and twice more in Locke's buffer (without MgCl<sub>2</sub> for glutamate experiments, or with 1 mM MgCl<sub>2</sub> for KCl experiments), and placed them in 1 ml Locke's buffer (without or with MgCl<sub>2</sub> for glutamate and KCl experiments, respectively) in a chamber on an IX70 Olympus microscope. We illuminated the cells with a mercury lamp, neutral density filter and 440 nm/21 nm excitation filter. We acquired CFP and YFP emission image pairs (2 s integration time per channel, 10 s between image pairs) through a 455-nm dichroic mirror and filter wheel with 480 nm/30 nm and 530 nm/26 nm filters (CVI Laser) mounted parfocally in front of a cooled Apogee KX85 CCD (Apogee Instruments Inc.). The acquired CFP emission images represent CFP signals quenched by FRET if any, and are referred to hereafter as CC images. The acquired Venus-YFP emission images represent raw FRET signals, and are referred to hereafter as CY images. The ratio of background-corrected CC and CY signals is referred to as CC/CY; this is the 2-filter FRET signal that is shown in the figures. We added

glutamate and glycine (final concentrations of 50  $\mu$ M or as indicated and 10  $\mu$ M, respectively) or KCl (30 mM final concentration) where indicated. In experiments using the NMDA receptor antagonist MK-801, we added it 30 min before starting the experiment as well as throughout the imaging procedure. We calculated 2-filter FRET (CC/CY ratio) timecourses from acquired image series with image analysis software developed by the authors<sup>50</sup>, modified to permit the processing of these image datasets as described above. We normalized background-corrected fluorescence ratio timecourses to the average pre-stimulation CC/CY ratio values for each cell, calculated averages of cells within each field, and presented data as mean  $\pm$  s.e.m. or range of independent experiments as indicated. The number of cells used in all figures is shown in **Supplementary Table 1** online. We used the Student's two-tailed *t*-test for statistical analysis.

**Staining and quantification of active Rho/Rac in brain slices.** See ref. 15. We prepared cryotome coronal sections (20  $\mu$ m) from snap-frozen brain. We fixed sections with 4% paraformaldehyde/PBS for 15 min, rinsed with 0.2% Tween/PBS, quenched with 1.5% hydrogen peroxide in PBS for 30 min, blocked with 10% FBS in PBS for 1 h, incubated overnight at +4 °C in block solution with GST-Rhotekin-RBD (0.5  $\mu$ g ml<sup>-1</sup>), or GST-PAK-CRIB (0.5  $\mu$ g ml<sup>-1</sup>), or GST (0.5  $\mu$ g ml<sup>-1</sup>), or block solution alone. We then re-fixed incubated sections in 2% PFH in PBS for 10 min and incubated in rabbit anti-GST antibody (0.5  $\mu$ g ml<sup>-1</sup>, cat. no. PC53, Oncogene) in blocking solution for 12 h at +4 °C. We rinsed sections with PBS and incubated in biotinylated anti-rabbit secondary antibody (1:800, Sigma) for 60 min. We visualized the biotin with tyramide-FITC using the TSA-Plus Fluorescence Palette System Kit (PerkinElmer Life Sciences) according to the manufacturer's instructions and acquired images as described above. We calculated average image intensities with MicroCCD software (Diffraction Ltd.), taking the signal with GST as background and subtracting this from other images. The background-corrected signal intensity of the ipsilateral side was normalized to the background-corrected signal intensity of the contralateral side for both Rhotekin-RBD and PAK-CRIB, and mean  $\pm$  s.e.m. values were calculated from averaged data obtained from four brains. All animal work was approved by the Animal Care and Use Committee of the University of Kuopio and performed according to the guidelines of the National Institutes of Health for animal care. Full experimental details of the methods used are available in the **Supplementary Methods** online.

*Note: Supplementary information is available on the Nature Neuroscience website.*

## ACKNOWLEDGMENTS

We thank M. Matsuda (University of Tokyo), B.J. Mayer (University of Connecticut Health Center), A. Miyawaki, L.A. Quilliam (Indiana University School of Medicine), J.M. Kyriakis (Tufts University School of Medicine), A. Hall (University College London), S. van den Heuvel (Massachusetts General Hospital Cancer Center), T. Wieland (Universitätsklinikum Hamburg-Eppendorf), M. Negishi (US National Institute of Environmental Health Sciences), H.A. Singer (Albany Medical College), M. Jäättelä (Danish Cancer Society) and J. Ellenberg (European Molecular Biology Laboratory) for providing plasmids used in this study. This work was funded by grants from the Academy of Finland (grants 72446, 78232, 203520, 206903 and 110445), the EU 6<sup>th</sup> Framework programme, the AIVI graduate school, the K. Albin Johansson Foundation and the University of Kuopio. M.J.C. is an Academy of Finland researcher.

## AUTHOR CONTRIBUTIONS

All authors conducted experiments for this work and M.J.C. also wrote the manuscript.

## COMPETING INTERESTS STATEMENT

The authors declare no competing financial interests.

Published online at <http://www.nature.com/natureneuroscience>

Reprints and permissions information is available online at <http://npg.nature.com/reprintsandpermissions>

- Palmer, G.C. & Widzowski, D. Low affinity use-dependent NMDA receptor antagonists show promise for clinical development. *Amino Acids* **19**, 151–155 (2000).
- Kawasaki, H. *et al.* Activation and involvement of p38 mitogen-activated protein kinase in glutamate-induced apoptosis in rat cerebellar granule cells. *J. Biol. Chem.* **272**, 18518–18521 (1997).

3. Borsello, T. *et al.* A peptide inhibitor of c-Jun N-terminal kinase protects against excitotoxicity and cerebral ischemia. *Nat. Med.* **9**, 1180–1186 (2003).
4. Cao, J. *et al.* Distinct requirements for p38 $\alpha$  and JNK stress-activated protein kinases in different forms of apoptotic neuronal death. *J. Biol. Chem.* **279**, 35903–35913 (2004).
5. Coffey, E.T., Hongisto, V., Dickens, M., Davis, R.J. & Courtney, M.J. Dual roles for JNK in developmental and stress responses in cerebellar granule neurons. *J. Neurosci.* **20**, 7602–7613 (2000).
6. Björkblom, B. *et al.* Constitutively active cytoplasmic c-Jun N-terminal kinase 1 is a dominant regulator of dendritic architecture: role of microtubule-associated protein 2 as an effector. *J. Neurosci.* **25**, 6350–6361 (2005).
7. Tararuk, T. *et al.* JNK1 phosphorylation of SCG10 determines microtubule dynamics and axodendritic length. *J. Cell Biol.* **173**, 265–277 (2006).
8. Bazenet, C.E., Mota, M.A. & Rubin, L.L. The small GTP-binding protein Cdc42 is required for nerve growth factor withdrawal-induced neuronal death. *Proc. Natl. Acad. Sci. USA* **95**, 3984–3989 (1998).
9. Linseman, D.A. *et al.* An essential role for Rac/Cdc42 GTPases in cerebellar granule neuron survival. *J. Biol. Chem.* **276**, 39123–39131 (2001).
10. Marinissen, M.J., Chiariello, M. & Gutkind, J.S. Regulation of gene expression by the small GTPase Rho through the ERK6 (p38 gamma) MAP kinase pathway. *Genes Dev.* **15**, 535–553 (2001).
11. Ramakers, G.J. Rho proteins, mental retardation and the cellular basis of cognition. *Trends Neurosci.* **25**, 191–199 (2002).
12. Lehmann, M. *et al.* Inactivation of Rho signaling pathway promotes CNS axon regeneration. *J. Neurosci.* **19**, 7537–7547 (1999).
13. Schwab, M.E. Nogo and axon regeneration. *Curr. Opin. Neurobiol.* **14**, 118–124 (2004).
14. Zhou, Y. *et al.* Nonsteroidal anti-inflammatory drugs can lower amyloidogenic A $\beta$ 42 by inhibiting Rho. *Science* **302**, 1215–1217 (2003).
15. Li, Z., Aizenman, C.D. & Cline, H.T. Regulation of rho GTPases by crosstalk and neuronal activity *in vivo*. *Neuron* **33**, 741–750 (2002).
16. Benink, H.A. & Bement, W.M. Concentric zones of active RhoA and Cdc42 around single cell wounds. *J. Cell Biol.* **168**, 429–439 (2005).
17. Wilde, C., Genth, H., Aktories, K. & Just, I. Recognition of RhoA by *Clostridium botulinum* C3 exoenzyme. *J. Biol. Chem.* **275**, 16478–16483 (2000).
18. Karnoub, A.E., Symons, M., Campbell, S.L. & Der, C.J. Molecular basis for Rho GTPase signaling specificity. *Breast Cancer Res. Treat.* **84**, 61–71 (2004).
19. Ren, X.D., Kiosses, W.B. & Schwartz, M.A. Regulation of the small GTP-binding protein Rho by cell adhesion and the cytoskeleton. *EMBO J.* **18**, 578–585 (1999).
20. Kjoller, L. & Hall, A. Signaling to Rho GTPases. *Exp. Cell Res.* **253**, 166–179 (1999).
21. Sander, E.E. *et al.* Matrix-dependent Tiam1/Rac signaling in epithelial cells promotes either cell-cell adhesion or cell migration and is regulated by phosphatidylinositol 3-kinase. *J. Cell Biol.* **143**, 1385–1398 (1998).
22. Yoshizaki, H. *et al.* Activity of Rho-family GTPases during cell division as visualized with FRET-based probes. *J. Cell Biol.* **162**, 223–232 (2003).
23. Reid, T. *et al.* Rhotekin, a new putative target for Rho bearing homology to a serine/threonine kinase, PKN, and rhophilin in the rho-binding domain. *J. Biol. Chem.* **271**, 13556–13560 (1996).
24. Wennerberg, K. *et al.* RhoG signals in parallel with Rac1 and Cdc42. *J. Biol. Chem.* **277**, 47810–47817 (2002).
25. Genth, H. *et al.* Entrapment of Rho ADP-ribosylated by *Clostridium botulinum* C3 exoenzyme in the Rho-guanine nucleotide dissociation inhibitor-1 complex. *J. Biol. Chem.* **278**, 28523–28527 (2003).
26. Courtney, M.J., Lambert, J.J. & Nicholls, D.G. The interactions between plasma membrane depolarization and glutamate receptor activation in the regulation of cytoplasmic free calcium in cultured cerebellar granule cells. *J. Neurosci.* **10**, 3873–3879 (1990).
27. Chen, J.C., Zhuang, S., Nguyen, T.H., Boss, G.R. & Pilz, R.B. Oncogenic Ras leads to Rho activation by activating the mitogen-activated protein kinase pathway and decreasing Rho-GTPase-activating protein activity. *J. Biol. Chem.* **278**, 2807–2818 (2003).
28. Hart, M.J. *et al.* Direct stimulation of the guanine nucleotide exchange activity of p115 RhoGEF by G $\alpha$ 13. *Science* **280**, 2112–2114 (1998).
29. Nakazawa, T. *et al.* p250GAP, a novel brain-enriched GTPase-activating protein for Rho family GTPases, is involved in the N-methyl-D-aspartate receptor signaling. *Mol. Biol. Cell* **14**, 2921–2934 (2003).
30. Gallagher, E.D., Gutowski, S., Sternweis, P.C. & Cobb, M.H. RhoA binds to the amino terminus of MEKK1 and regulates its kinase activity. *J. Biol. Chem.* **279**, 1872–1877 (2004).
31. Zong, H., Raman, N., Mickelson-Young, L.A., Atkinson, S.J. & Quilliam, L.A. Loop 6 of RhoA confers specificity for effector binding, stress fiber formation, and cellular transformation. *J. Biol. Chem.* **274**, 4551–4560 (1999).
32. Ishizaki, T. *et al.* Pharmacological properties of Y-27632, a specific inhibitor of rho-associated kinases. *Mol. Pharmacol.* **57**, 976–983 (2000).
33. Arakawa, Y. *et al.* Control of axon elongation via an SDF-1 $\alpha$ /Rho/mDia pathway in cultured cerebellar granule neurons. *J. Cell Biol.* **161**, 381–391 (2003).
34. Marinissen, M.J. *et al.* The small GTP-binding protein RhoA regulates c-jun by a ROCK-JNK signaling axis. *Mol. Cell* **14**, 29–41 (2004).
35. Coffey, E.T. *et al.* JNK2/3 is specifically activated by stress, mediating c-jun activation, in the presence of constitutive JNK1 activity in cerebellar neurons. *J. Neurosci.* **22**, 4335–4345 (2002).
36. Jeon, S. *et al.* RhoA and Rho kinase-dependent phosphorylation of moesin at Thr-558 in hippocampal neuronal cells by glutamate. *J. Biol. Chem.* **277**, 16576–16584 (2002).
37. Sattler, R., Xiong, Z., Lu, W.Y., MacDonald, J.F. & Tymianski, M. Distinct roles of synaptic and extrasynaptic NMDA receptors in excitotoxicity. *J. Neurosci.* **20**, 22–33 (2000).
38. Chalecka-Franaszek, E. & Chuang, D.M. Lithium activates the serine/threonine kinase Akt-1 and suppresses glutamate-induced inhibition of Akt-1 activity in neurons. *Proc. Natl. Acad. Sci. USA* **96**, 8745–8750 (1999).
39. Didenko, V.V. *et al.* Caspase-3-dependent and -independent apoptosis in focal brain ischemia. *Mol. Med.* **8**, 347–352 (2002).
40. Fukuda, T., Wang, H., Nakanishi, H., Yamamoto, K. & Kosaka, T. Novel non-apoptotic morphological changes in neurons of the mouse hippocampus following transient hypoxic-ischemia. *Neurosci. Res.* **33**, 49–55 (1999).
41. Yu, S.W., Wang, H., Dawson, T.M. & Dawson, V.L. Poly(ADP-ribose) polymerase-1 and apoptosis inducing factor in neurotoxicity. *Neurobiol. Dis.* **14**, 303–317 (2003).
42. Sohn, S., Kim, E.Y. & Gwag, B.J. Glutamate neurotoxicity in mouse cortical neurons: atypical necrosis with DNA ladders and chromatin condensation. *Neurosci. Lett.* **240**, 147–150 (1998).
43. Csernansky, C.A., Canzoniero, L.M., Sensi, S.L., Yu, S.P. & Choi, D.W. Delayed application of aurointricarboxylic acid reduces glutamate-induced cortical neuronal injury. *J. Neurosci. Res.* **38**, 101–108 (1994).
44. Lobner, D. & Choi, D.W. Preincubation with protein synthesis inhibitors protects cortical neurons against oxygen-glucose deprivation-induced death. *Neuroscience* **72**, 335–341 (1996).
45. Gwag, B.J. *et al.* Slowly triggered excitotoxicity occurs by necrosis in cortical cultures. *Neuroscience* **77**, 393–401 (1997).
46. Legos, J.J. *et al.* SB 239063, a novel p38 inhibitor, attenuates early neuronal injury following ischemia. *Brain Res.* **892**, 70–77 (2001).
47. Dawson, V.L., Kizushi, V.M., Huang, P.L., Snyder, S.H. & Dawson, T.M. Resistance to neurotoxicity in cortical cultures from neuronal nitric oxide synthase-deficient mice. *J. Neurosci.* **16**, 2479–2487 (1996).
48. Huang, Z. *et al.* Effects of cerebral ischemia in mice deficient in neuronal nitric oxide synthase. *Science* **265**, 1883–1885 (1994).
49. Nagai, T., Yamada, S., Tominaga, T., Ichikawa, M. & Miyawaki, A. Expanded dynamic range of fluorescent indicators for Ca(2+) by circularly permuted yellow fluorescent proteins. *Proc. Natl. Acad. Sci. USA* **101**, 10554–10559 (2004).
50. Courtney, M.J., Åkerman, K.E. & Coffey, E.T. Neurotrophins protect cultured cerebellar granule neurons against the early phase of cell death by a two-component mechanism. *J. Neurosci.* **17**, 4201–4211 (1997).